Emulsification in Batch Emulsion Polymerization

M. F. KEMMERE, J. MEULDIJK, A. A. H. DRINKENBURG, A. L. GERMAN

Laboratory of Process Development, Eindhoven University of Technology, P.O. Box 513, 5600 MB Eindhoven, The Netherlands

Received 13 August 1998; accepted 10 June 1999

ABSTRACT: Dispersion of liquid–liquid systems is often applied in industrial processes such as extraction, suspension, and emulsion polymerization. The influence of emulsification of the monomer in the aqueous phase on the course and outcome of the batch emulsion polymerization of styrene has been studied. A visual criterion was applied for determining the lowest impeller speed for sufficient emulsification (N^*). It appeared that in polymerization experiments under the same conditions, N^* was the critical value above which no further increase in polymerization rate was observed. Using a turbine impeller instead of a pitched blade impeller as well as using a larger impeller diameter provides better emulsification at constant power input. The results indicate that scale-up with constant impeller tip speed is most appropriate in case of a turbine impeller. © 1999 John Wiley & Sons, Inc. J Appl Polym Sci 74: 3225–3241, 1999

Key words: emulsification; emulsion polymerization; styrene, scale-up

INTRODUCTION

Emulsion polymerization is a free radical polymerization in a heterogeneous reaction system. During batch emulsion polymerization of sparsely water soluble monomers such as styrene, three different time-separated intervals can be distinguished: particle nucleation (I), and polymerization with (II) and without (III) monomer droplets present.[1,2] At the beginning of the polymerization the monomer is mainly present in droplets being dispersed in the continuous phase. The monomer droplets serve as monomer reservoirs. A typical size of the monomer droplets is about 5 μm.[3]

Stirring is necessary during emulsion polymerization to keep the monomer phase properly dispersed. If the dispersion is not sufficient, mass transfer limitation of the monomer from the monomer phase to the particle phase may occur. Such mass transfer limitation negatively affects the polymerization process. The quality of emulsification of the monomer is important for the product properties of the ultimate latex product in terms of, for example, particle size (distribution).

This article combines the current understanding of emulsification with the emulsion polymerization process. Key questions are: What is the minimum power input due to stirring to maintain a proper dispersion of the monomer in the aqueous phase? How sensitive is the course and outcome of the emulsion polymerization process to emulsification? Which scale-up rule is adequate for the process?

EMULSIFICATION

Emulsification is the process of making an emulsion by mechanical agitation of a system, containing two approximately immiscible liquids and in many cases a surfactant.[4] As a result of the Gibbs energy necessary to maintain large oil/water surface areas, emulsions are thermodynamically not stable. The droplet size distribution is governed by a dynamic equilibrium between break up and coalescence of the droplets.

Correspondence to: M. F. Kemmere.

Journal of Applied Polymer Science, Vol. 74, 3225–3241 (1999)
 CCC 0021-8995/99/133225-17

Droplet Size

In a stirred dispersion, deformation of the droplets occurs as a result of the shear forces in the turbulent flow field. The droplets endure viscous shear stress, pressure variations along their surface and turbulent velocity fluctuations.[5,6] Breakup occurs if the hydrodynamic forces exceed the stabilizing forces originating from the interfacial tension and drop viscosity.[7] Deformation and breakup is characterized by the Weber number, which is defined as the ratio of kinetic energy and surface energy. Breakup occurs if the Weber number exceeds a critical value.

$$We = \frac{\rho_c u^2(d) d}{\sigma} \tag{1}$$

where ρ_c, d, and σ, respectively, stand for the density of the continuous phase, droplet size, and interfacial tension. The mean square of relative velocity fluctuations between two diametrically opposite points on the surface of droplets is represented by u^2.[6]

In emulsion polymerization, monomer droplet sizes are usually within the Kolmogorov microscale of turbulence. In the case of isotropic homogeneous turbulence, the viscous shear forces are then the dominant forces for deformation. In the case described above, the largest stable droplet size before breakup occurs is given by:[6,8]

$$d_{\max} = C'\left(\frac{\sigma}{\mu_c}\right)\left(\frac{v_c}{\varepsilon_{\mathrm{av}}}\right)^{0.5}\Phi\left(\frac{\mu_d}{\mu_c}\right) \tag{2}$$

in which μ_c, μ_d, μ_c, and $\varepsilon_{\mathrm{av}}$, respectively, represent the dynamic viscosity of continuous phase and dispersed phase, the kinematic viscosity of continuous phase and the mean energy dissipation. Φ is a function of the ratio of the dynamic viscosity of the continuous and the dispersed phase.

Coalescence of droplets in a turbulent liquid–liquid system is affected by the ratio of continuous and dispersed phase, the hydrodynamic forces, as well as the physicochemical properties of both phases and of the interface.[9] The coalescence rate is determined by the collision frequency and coalescence efficiency. The latter strongly depends on the thickness and physicochemical properties of the thin liquid film between two approaching droplets. According to Ivanov,[10] the rate of film thinning and the critical film thickness at which film rupture occurs, are both influenced by the emulsifier present at the interface of the droplets.

For monomer droplets smaller than the Kolmogorov microscale, the smallest stable droplet size before coalescence occurs can be given by:[11]

$$d_{\min} = C''\left(\frac{F}{\mu_c}\right)^{0.5}\left(\frac{v_c}{\varepsilon_{\mathrm{av}}}\right)^{0.25} \tag{3}$$

in which F represent the interaction force between two droplets.

Because a pseudosteady state is reached for equal rates of breakage and coalescence, the average monomer droplet size in a particular emulsion system lies between the droplet size calculated with eq. (3) and that calculated with eq. (2).

Lowest Impeller Speed for Sufficient Emulsification

The degree of emulsification in a dispersion is often expressed in the lowest impeller speed N^*, necessary for sufficient emulsification of a liquid–liquid system. This stirrer speed has been defined by Skelland and Seksaria[12] as the lowest impeller speed just sufficient to completely disperse one liquid into the other, so that no clear liquid is observed at either the top or the bottom of the stirred vessel. In the literature, empirical relations have been developed to predict N^*. Variables include physical properties of the liquid–liquid system, impeller diameter, and impeller type.

Van Heuven and Beek[13] developed empirical relation (4) for water/hexane and water/octanol mixtures. Relation (4) is based on the results of emulsification experiments in stirred tanks of various scales equipped with Rushton turbine impellers. Volume fractions of the dispersed phase up to 40 vol% have been investigated.

$$N^* = 3.28\,\frac{(g\Delta\rho)^{0.385}\mu_c^{0.0769}\sigma^{0.0769}(1 + 2.5\phi_v)^{0.897}}{D^{0.769}\rho_M^{0.538}} \tag{4}$$

Skelland and coworkers[14,15] have reported eq. (5) based on experiments with various impeller types and four different liquid systems on 7.64 dm^3 tank scale:

$$N^* = C'''\left(\frac{T}{D}\right)^{\alpha}\frac{(g\Delta\rho)^{0.416}\mu_M^{0.084}\sigma^{0.042}\phi_v^{0.053}}{D^{0.71}\rho_M^{0.542}} \tag{5}$$

where ϕ_v, μ_M, ρ_M, and $\Delta\rho$ stand for the volume fraction of the dispersed phase, the dynamic viscos-

ity of the mixture, the density of the mixture, and the difference in density between the continuous and the dispersed phase, respectively. D and T are the impeller and vessel diameter, respectively.

Equations (2), (3), (4), and (5) show that emulsification is influenced by the equipment and energy dissipated into the liquid mixture as well as the physicochemical properties of the system.

ENERGY DISSIPATION

The energy dissipation in a liquid–liquid system depends on the tank configuration, scale of operation, impeller speed, impeller geometry, and the kind of liquids used. The power (P) transferred into the liquid mixture can be determined from the torque on the impeller shaft [see eq. (6)], or can be estimated using the dimensionless power number (N_p) [see eq. (7)]. The power number depends on the tank configuration, the flow pattern, impeller type and speed, and the physical properties of the mixture. The Reynolds number [see eq. (8)], is an important parameter to characterize the flow in a stirred vessel. In the turbulent flow regime, the power number appears to be mainly dependent of the impeller type and the geometrical arrangement.[16]

$$P = 2\pi N_i T_q \tag{6}$$

$$P = N_p \rho_M N_i^3 D^5 \tag{7}$$

$$\mathrm{Re} = \frac{\rho_M N_i D^2}{\mu_M} \tag{8}$$

in which N_i, T_q, and N_p stand for the impeller speed, torque, and power number, respectively.

The mean energy dissipation $\varepsilon_{\mathrm{av}}$, the power input per unit of mass, is given by:

$$\varepsilon_{\mathrm{av}} = \frac{P}{M_M} \tag{9}$$

in which M_M is the mass of the mixture.

Because the critical droplet size for breakup and coalescence is proportional to the mean energy dissipation to the power -0.5 and -0.25, respectively [see eqs. (2) and (3)], the mean droplet size for simultaneously breakup and coalescence of droplets in an emulsion is expected to be for exact Rushton geometry ($M_M \propto V_M \propto T^3 \propto D^3$):

$$d \propto (\varepsilon_{\mathrm{av}})^{-\beta} \propto \left(\frac{D^5 N_i^3}{D^3}\right)^{-\beta} = (D^2 N_i^3)^{-\beta} \quad \text{with } 0.25 \le \beta \le 0.5 \tag{10}$$

The Rushton turbine impeller generates a radial circulation profile, while a pitched blade impeller gives an axial circulation (see Fig. 1). During one circulation time, an element of emulsified fluid is exposed to regions with different energy dissipation.[17] The distribution of the power transferred into the mixture by the impeller depends strongly on the geometrical arrangement, meaning the reactor dimensions in combination with the location, type, and diameter of the impeller. As a result of the difference between shear rates and energy dissipation in the impeller region and circulation zone of the vessel,[18,19] breakup is likely to prevail near the impeller where shear rates and energy dissipation are high. According to Schäfer et al.,[20] the trailing vortices near the impeller blades are the major flow mechanism for phenomena such as drop break up. Coalescence is expected to be dominant in the circulation region of the vessel where shear rates are relatively low.[11] The circulation time of the liquid in the vessel is defined as follows:[21]

$$t_c = \frac{V_M}{N_c D^3 N_i} \tag{11}$$

where N_c is the circulation number.

Scale-Up Rules

In general, to translate a process from laboratory scale to larger scale, a choice between the following scale-up rules can be considered: (1) constant impeller speed: N_i = constant; (2) constant impeller tip speed: $N_i D$ = constant; (3) constant circulation time: $t_c \propto (D^3/N_i D^3) = N_i^{-1}$ = constant; (4) constant Reynolds number: $\mathrm{Re} \propto N_i D^2$ = constant; (5) constant power input: $P \propto N_i^3 D^5$ = constant; and (6) constant mean energy dissipation: $\varepsilon_{\mathrm{av}} \propto (N_i^3 D^5/D^3) \propto N_i^3 D^2$ = constant.

Several authors investigated the scale-up of emulsification processes. Esch et al.[22] suggested that scaling up of reactors for heterogeneous liquid systems requires a constant batch mixing time. The batch mixing time is the product of the circulation time and the number of cycles required to obtain a uniform concentration of dispersed phase throughout the vessel. Esch et al.[22] use the relationship $N_i D^{0.15}$ = constant to predict

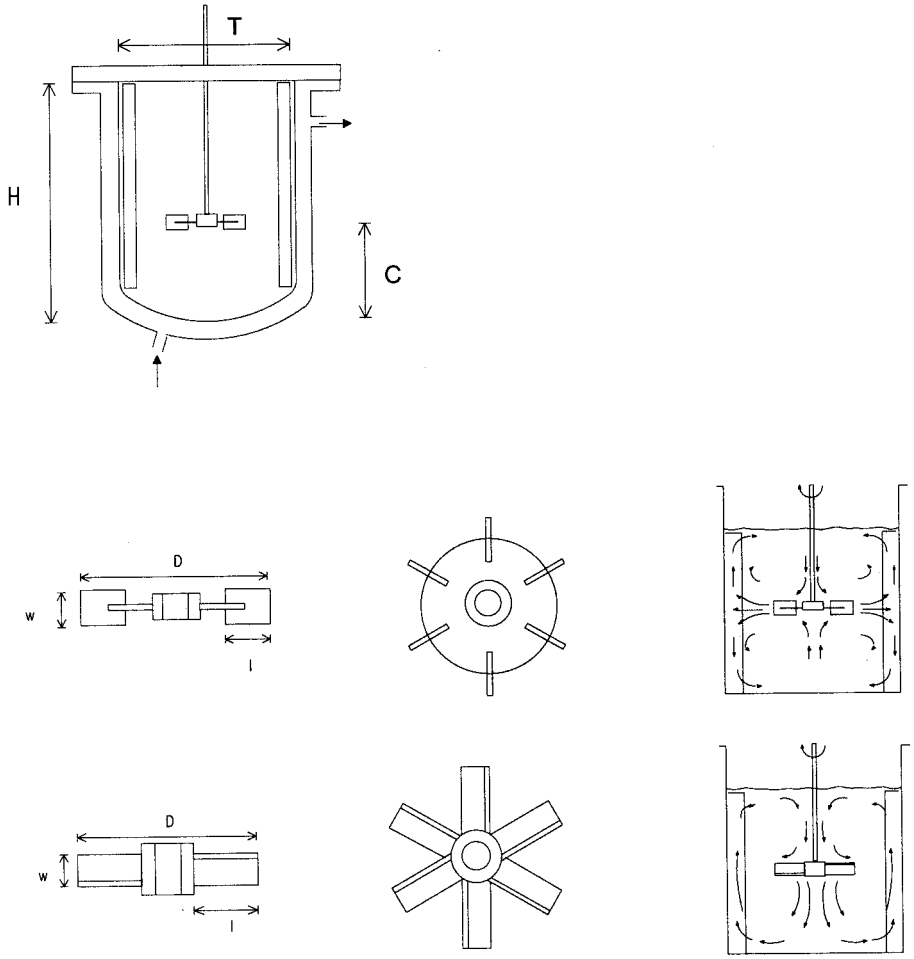

Figure 1 Schematic view of the Rushton polymerization and visualization vessels, turbine, and 45° pitched six-bladed impellers with corresponding flow patterns.

N^* for operation on different scales. Van Heuven and Beek[13] reported scale-up rules for both droplet size and N^*. According to the results of Van Heuven en Beek, the droplet size will be constant by scaling up on the basis of a constant mean energy dissipation. However, the impeller speed N^* is not completely constant during scale-up with constant mean energy dissipation [$N_i\ D^{0.77}$ = constant—see eq. (4)—instead of $N_i\ D^{2/3}$ = constant]. According to Skelland and Ramsay,[14] the scale-up rule of constant energy dissipation for full geometric similarity (i.e., T/D is constant) and constant physical properties is not valid for finding of N^* [$N_i\ D^{0.71}$ = constant; see eq. (5)].

According to Zhou and Kresta,[23,24] both energy dissipation and flow are important considering the scale-up of liquid–liquid dispersions. They suggested that the mean drop size distribution is better correlated to the maximum energy dissipation rate than to either the average power input per unit mass of dispersion or the impeller tip speed.

Notice that emulsification is just one aspect of the scale-up of the emulsion polymerization process; other matters of concern are, for example, reaction rate, colloidal stability, and reactor fouling.

PHYSICOCHEMICAL PROPERTIES OF THE SYSTEM

Surfactant

The emulsifier used in the system affects both emulsification of the monomer and polymerization. The present study reveals the effects of the anionic surfactant sodium dodecyl sulfate. The type as well as the concentration of surfactant are important; this contribution only discusses the

latter. Hoedemakers[25] observed considerable differences in emulsification for styrene/water emulsions on using rosin acid soap or sodium dodecyl sulfate as emulsifier.

The effect of the surfactant concentration on emulsification is twofold. Emulsifier lowers the interfacial tension, making the shear generated by the stirring device more effective to break-up droplets. Additionally, surfactant retards the film thinning between two approaching droplets. This results in a lower coalescence efficiency and coalescence rate. Effects of adsorbed emulsifier on the droplet surface are likely to be more important when neighboring interfaces are close, which is the case for high monomer fractions.[17]

The total effect of surfactant in the emulsion system will be a decreasing droplet size when the emulsifier concentration increases. Above the critical micelle concentration, the tension does not change any more with increasing the emulsifier concentration. In that case, the breakup is less sensitive to a change in emulsifier concentration.[17]

Surfactant also affects the emulsion polymerization itself. For case 2 kinetics, which is generally obeyed by the emulsion polymerization of styrene, Smith and Ewart[2] derived the following relation for the particle number (N_{part}) and polymerization rate (R_p):

$$N_{\text{part}} \propto R_p \propto C_{I0}^{0.4}(C_{E,\text{ov}} - C_{\text{CMC}})^{0.6} C_{M0}^{0} \qquad (12)$$

where C_{I0}, $C_{E,\text{ov}}$ and C_{M0} stand for the concentrations of initiator, emulsifier and monomer, respectively. C_{CMC} is the critical micelle concentration.

Increasing the emulsifier concentration results in a higher polymerization rate. Consequently, the time constant of monomer transfer from the monomer droplets through the aqueous phase to the growing polymer particles should be sufficiently high to avoid any limitations of the polymerization rate. The monomer water surface area have to be large enough to ensure that the polymerization rate will be governed by intrinsic kinetics.

Monomer

Both type and concentration of monomer have impact on the emulsification of the system. In this study, only one type of monomer have been investigated.

An increasing fraction of monomer in the system increases the collision frequency of the droplets, and consequently, the coalescence rate. The emulsion viscosity and the impact of adsorbed surfactant on the droplet surface also change, due to the enhanced mutual interaction of the droplets at high monomer fraction in the system.

According to eq. (12), the monomer concentration does not affect the reaction rate of the emulsion polymerization.

Reaction Temperature

The temperature affects both emulsification and polymerization. An increase in temperature can produce opposite effects on droplet size.[17] Due to a higher temperature, the internal phase viscosity decreases, enhancing the droplet break up rate. On the other hand, a higher temperature reduces the surfactant adsorption, increasing the interfacial tension. A high interfacial tension favors coalescence at the expense of the break up of droplets. Depending on the system used and the magnitude of the temperature change, one of both effects prevails.

The emulsion polymerization is affected by temperature, because both the initiator decomposition rate and propagation rate are dependent on temperature according to the Arrhenius equation. Because higher temperatures result in higher polymerization rates, the requirements for sufficient emulsification of the monomer are higher.

EXPERIMENTAL

Two baffled stainless steel polymerization reactors geometry of 1.85 and 7.48 dm^3 with Rushton were used. In each vessel a Rushton turbine impeller and a 45° pitched six-blade impeller of half and one-third of the vessel diameter were used. The clearance was half of the vessel diameter. The width of the four baffles was 10% of the vessel diameter. The power number of each impeller was determined from torque measurements in glycerol/water mixtures.

Figure 1 shows a schematic view of the reactor configuration as well as the impellers used for this study. Table I gives the dimensions of the equipment as well as the characteristic power number and circulation number of all impellers used in this study.

The torque exerted on the impeller was measured by a Staiger Mohilo torque meter, installed between the motor and the impeller shaft. On the 1.85 and 7.48 dm^3 scale, two torque meters with varying ranges of respectively 0.1 and 1 Nm were used.

Table I Dimensions of the Rushton Polymerization and Visualization Vessels, Turbine, and 45° Pitched Six-Blade Impellers

Dimensions of Polymerization and Visualization Vessels (mm)		
Scale (dm^3)	1.85	7.48
Internal diameter T	133	212
Height H_{fill}	133	212
Height impeller C	66	106
Diameter baffles	13	20
Thickness baffles	1.5	2

Dimensions of Six-Bladed Rushton Turbine Impeller (mm)				
Scale (dm^3)	1.85		7.48	
Impeller diameter D	T/3 = 44	T/2 = 66	T/3 = 71	T/2 = 106
Blade width w	9	13	14	21
Blade length l	11	16	18	26
Blade thickness	1.5	1.5	1.5	1.5
Disk diameter	33	50	53	79
Disk thickness	1.5	1.5	1.5	1.5
Shaft diameter	7	7	10	10
Shaft holder diameter	12	12	18	27
Power number (−)	5.2	4.9	4.4	4.4
Circulation number[21] (−)	2.3	2.3	2.3	2.3

Dimensions of 45° Pitched Downflow Six-Blade Impeller (mm)				
Scale (dm^3)	1.85		7.48	
Impeller diameter D	T/3 = 44	T/2 = 66	T/3 = 71	T/2 = 106
Blade width w	9	13	14	21
Blade length l	17	25	26	42
Blade thickness	1.5	1.5	1.5	1.5
Shaft diameter	7	7	10	10
Shaft holder diameter	12	12	18	27
Power number (−)	2.6	2.1	1.6	1.3
Circulation number[21] (−)	1.4	1.4	1.4	1.4

Droplet Size Versus Lowest Impeller Speed for Sufficient Emulsification

In our laboratory two methods for droplet size measurement in emulsion systems were applied: off-line laser diffraction spectrometry using a Malvern 2600HSL particle sizer,[25] and an on-line laser back-scattering technique, using a Partec 100.[26] Both methods have shown limitations for the investigation of emulsification. Applying the off-line method, samples are strongly diluted, approaching the water solubility of the monomer. Because of this strong dilution, the droplets may dissolve partially in the aqueous phase. Besides that, the samples have to be stable during a period of at least 10 min, which is not very likely considering the low internal viscosity of the monomer droplets. The results obtained by Hoedemakers deviate from results reported in literature.[25,27]

The on-line method could not give reliable quantitative information on droplet sizes.[26] However, it was possible to observe trends in droplet size as a function of energy dissipation and monomer fraction. The major drawback of this method is that it is impossible to measure droplet sizes in liquid–liquid systems with surfactant. In those systems the monomer droplets are generally too small to be measured with this technique.

We found that the visual criterion for proper emulsification based on N^* was more reliable than a criterion based on drop size measurement.

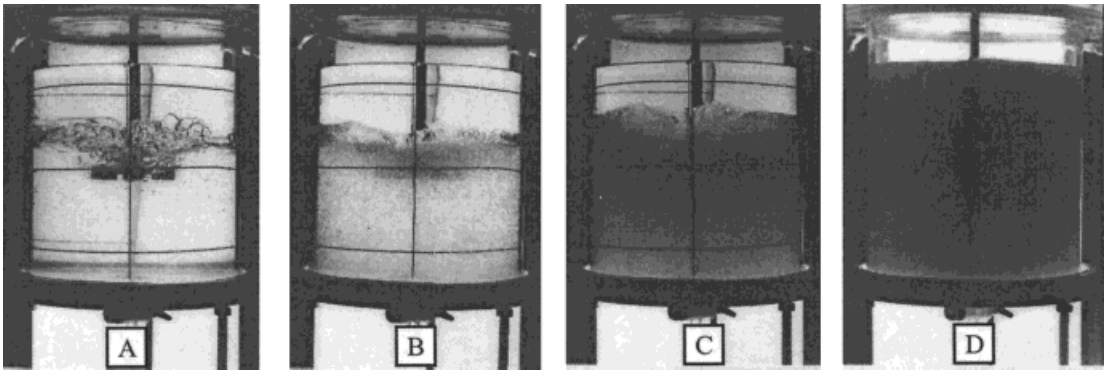

Figure 2 Still camera pictures of visualization experiments to determine N^* needed for sufficient emulsification. $C_{E,ov} = 0$ kmol/m_w^3, $T_r = 20°C$, $\phi_M = 0.27$, Rushton turbine impeller with $D = 1/3\ T$ on a 7.48 dm^3 scale. Stirrer speed: (A) 100 rpm; (B) 150 rpm; (C) 200 rpm; (D) 320 rpm = N^*.

Therefore, this visual criterion was used throughout.

Visualization Experiments

The influence of emulsifier concentration, monomer-to-water ratio, temperature, and mixing conditions on emulsification were studied in glass vessels, which have the same geometry as the polymerization reactors. A visual criterion was used to determine the lowest impeller speed for sufficient emulsification (N^*) (see Fig. 2). The stirrer speed was increased stepwise. After each speed increment the system was allowed to reach the new pseudosteady state. The impeller speed at which the clear liquid just disappeared was N^*. No hysteresis was observed.

Polymerization Experiments

Ab initio emulsion polymerization experiments of styrene with several mixing conditions (reactor scale, impeller speed, type, and diameter) were performed. The reaction temperatures were 50.0 $\pm$ 0.5 and 75 $\pm$ 0.5°C, respectively. The pH was 10.5 in all cases. The recipe used is given in Table II.

Before the start of a polymerization, the reactor was charged with water, emulsifier, buffer, and monomer. The reaction mixture was stirred, heated up to the reaction temperature, and flushed with argon for 1 h to remove oxygen. The reaction was started by adding an aqueous initiator solution to the reactor. During the polymerization, samples were taken to determine the conversion (by gravimetry) and the particle size (distribution) using a JEOL 2000 FX Transmission Electron Microscope.

RESULTS AND DISCUSSION

Visualization Experiments

The stirrer speeds N^* as determined by visualization experiments on 1.85 dm^3 scale, have been collected in Table III. The results show that the influence of emulsifier on N^* was twofold. The difference between N^* for water/styrene mixtures with and without emulsifier was considerable (e.g., 550 rpm, respectively, 320 rpm for the given examples; see Experiments 1 and 2). Increasing the emulsifier concentration from 0.01 to 0.02 kmol/m_w^3 only slightly influenced N^* (see, e.g., Experiments 5 and 6). These results support the explanation by Salager et al.,[17] that for emulsifier concentrations above the critical micelle concentration no significant influence of emulsifier concentration on the emulsification process can be expected.

Table II Recipe Used for the *Ab Initio* Emulsion Polymerization Experiments of Styrene

Ingredient	Concentration (kmol/m_w^3)
Styrene	3.20
Sodium persulfate	$10.0 \cdot 10^{-3}$
Sodium dodecyl sulfate	$10.0 \cdot 10^{-3}/20.0 \cdot 10^{-3}$
Sodium carbonate	$9.45 \cdot 10^{-3}$

Table III N^* Determined with Visualization Experiments on 1.85 dm^3 Scale

Exp.	Impeller Type	$C_{E,ov}$ (kmol/m_w^3)	T_r (°C)	ϕ_M (−)	N^* (rpm)	T_q (Nm)	$\varepsilon_{av,m}$ (W/kg)	$\varepsilon_{av,c}$ (W/kg)	t_c (s)
1	1/3 T turbine	0	20.0	0.25	550	—	—	0.36	1.0
2	1/3 T turbine	0.01	20.0	0.25	320	—	—	0.070	1.8
3	1/3 T turbine	0	20.0	0.50	550	—	—	0.36	1.0
4	1/3 T turbine	0.08	20.0	0.50	330	—	—	0.077	1.7
5	1/3 T turbine	0.01	50.0	0.25	360	—	—	0.10	1.6
6	1/3 T turbine$^+$	0.02	50.0	0.25	390	0.010	0.22	0.13	1.5
7	1/3 T turbine	0.01	50.0	0.50	335	0.015	0.30	0.081	1.7
8	1/3 T turbine	0.08	50.0	0.50	345	0.016	0.33	0.088	1.6
9	1/3 T turbine	0.01	75.0	0.25	370	0.0074	0.16	0.11	1.5
10	1/2 T turbine	0.01	20.0	0.25	115	0.015	0.10	0.023	1.5
11	1/2 T turbine	0.08	20.0	0.50	115	0.018	0.13	0.023	1.5
12	1/2 T turbine	0.01	50.0	0.25	130	0.018	0.14	0.034	1.3
13	1/2 T turbine$^+$	0.02	50.0	0.25	160	0.0088	0.078	0.063	1.0
14	1/2 T turbine	0.08	50.0	0.50	140	0.018	0.15	0.042	1.2
15	1/2 T turbine	0.01	75.0	0.25	145	0.0095	0.081	0.047	1.2
16	1/3 T pitch b.	0.01	20.0	0.25	490	0.0092	0.26	0.13	1.9
17	1/3 T pitch b.	0.08	20.0	0.50	510	0.0092	0.28	0.14	1.8
18	1/3 T pitch b.	0.01	50.0	0.25	580	0.0083	0.28	0.21	1.6
19	1/3 T pitch b.$^+$	0.02	50.0	0.25	720	0.011	0.45	0.40	1.3
20	1/3 T pitch b.	0.08	50.0	0.50	620	0.0091	0.34	0.26	1.5
21	1/3 T pitch b.	0.01	75.0	0.25	710	0.014	0.58	0.38	1.3
22	1/2 T pitch b.	0.01	20.0	0.25	180	0.0046	0.059	0.038	1.5
23	1/2 T pitch b.	0.08	20.0	0.50	260	0.011	0.17	0.12	1.1
24	1/2 T pitch b.	0.01	50.0	0.25	195	0.0053	0.061	0.049	1.4
25	1/2 T pitch b.$^+$	0.02	50.0	0.25	235	0.010	0.13	0.085	1.2
26	1/2 T pitch b.	0.08	50.0	0.50	270	0.0082	0.13	0.13	1.0
27	1/2 T pitch b.	0.01	75.0	0.25	210	0.0089	0.11	0.061	1.3

An increase in the monomer weight fraction from 0.25 to 0.50 did not change N^* under further equal circumstances (see, e.g., Experiments 1 and 3). All systems used in this study have rather high monomer concentrations. Apparently the emulsification was not significantly sensitive to variations in monomer concentration for systems at the monomer concen-

Table IV N^* Determined with Visualization Experiments on a 7.48 dm^3 Scale with $\phi_m = 0.25$

Exp.	Impeller Type	$C_{E,ov}$ (kmol/m_w^3)	T_r (°C)	N^* (rpm)	T_q (Nm)	$\varepsilon_{av,m}$ (W/kg)	$\varepsilon_{av,c}$ (W/kg)	t_c (s)
28	1/3 T turbine	0	20.0	235	0.013	0.044	0.064	2.3
29	1/3 T turbine	0.01	20.0	155	0.013	0.029	0.018	3.5
30	1/3 T turbine	0.01	50.0	205	0.013	0.039	0.042	2.7
31	1/3 T turbine$^+$	0.02	50.0	225	0.024	0.075	0.056	2.4
32	1/2 T turbine	0.01	20.0	70	0.018	0.018	0.013	2.3
33	1/2 T turbine	0.01	50.0	85	0.018	0.022	0.022	1.9
34	1/2 T turbine$^+$	0.02	50.0	105	0.030	0.054	0.042	1.6
35	1/3 T pitch b.	0.01	20.0	285	0.018	0.074	0.041	2.7
36	1/3 T pitch b.	0.01	50.0	420	0.018	0.11	0.13	2.3
37	1/3 T pitch b.$^+$	0.02	50.0	550	0.037	0.28	0.30	1.7
38	1/2 T pitch b.	0.01	20.0	100	0.017	0.025	0.011	3.1
39	1/2 T pitch b.	0.01	50.0	115	0.017	0.028	0.016	2.1
40	1/2 T pitch b.$^+$	0.02	50.0	160	0.027	0.060	0.044	1.6

Table V Various Scale-Up Rules of N^* Compared with the Experimentally Observed Values

Impeller Type	$C_{E,ov}$ (kmol/m_w^3)	T_r (°C)	N^*(exp) 1.85 dm^3 (rpm)	N^*(exp) 7.48 dm^3 (rpm)	N^* Esch (rpm)	N^* Skelland (rpm)	N^* Heuven (rpm)	N^* Tip Speed (rpm)	N^* Re (rpm)	N^* P (rpm)	N^* ε_{av} (rpm)
1/3 T turbine	0.01	20.0	320	155	298	228	221	198	123	144	233
1/3 T turbine	0.01	50.0	360	205	335	256	249	223	138	162	262
1/3 T turbine$^+$	0.02	50.0	390	225	363	278	270	241	150	177	283
1/2 T turbine	0.01	20.0	115	70	107	82	80	72	45	52	84
1/2 T turbine	0.01	50.0	130	85	121	93	90	81	50	59	95
1/2 T turbine$^+$	0.02	50.0	160	105	149	114	111	100	62	73	117
1/3 T pitch b.	0.01	20.0	490	285	456	349	339	304	188	221	356
1/3 T pitch b.	0.01	50.0	580	420	540	413	401	359	223	261	422
1/3 T pitch b.$^+$	0.02	50.0	720	550	670	513	498	446	277	324	523
1/2 T pitch b.	0.01	20.0	180	100	168	129	125	112	70	82	131
1/2 T pitch b.	0.01	50.0	195	115	182	139	135	121	76	89	142
1/2 T pitch b.$^+$	0.02	50.0	235	160	219	168	163	146	91	107	171

All calculated values are on a 7.48 dm^3 scale.

tration level used. This result is in contrast with diluted systems in which the concentration of dispersed phase significantly influenced the emulsification.[9]

At higher temperature, a higher N^* for emulsification was found (see, e.g., Experiments 2 and 5). A possible explanation is that higher temperatures result in a higher interfacial tension. The opposite effect of a lower internal viscosity of the dispersed phase resulting from an increase in temperature, as described by Salager et al.,[17] appeared to be not significant for the dispersions investigated in this study. The monomer droplets have already a relatively low internal viscosity at low temperature.

Visualization experiments have also been carried out in the presence of latex particles. In Table III, these experiments are marked with $^+$. The results reveal that polymer particles increase N^* in all cases, but in particular, in the experiment with a pitched-blade impeller of $D = 1/3\ T$ (see Experiment 19).

In Table IV the values of N^*, determined on a 7.48 dm^3 scale with a monomer volume fraction of

Table VI N^* Calculated with the Empirical Equations Reported by van Heuven and Beek,[17] Eq. (4), and Skelland and Ramsay,[14] Eq. (5)

Impeller Type	Scale (dm^3)	ϕ_M (−)	Emulsifier	N^* (exp) (rpm)	$N^*_{eq\,4}$ (rpm)	$N^*_{eq\,5}$ (rpm)	Scale (dm^3)	ϕ_M (−)	Emulsifier	N^* (exp) (rpm)	$N^*_{eq\,4}$ (rpm)	$N^*_{eq\,5}$ (rpm)
1/3 T turbine	1.85	0.25	no	550	573	394	7.48	0.25	no	235	397	280
1/3 T turbine	1.85	0.25	yes	360	480	357	7.48	0.25	yes	205	333	254
1/3 T turbine	1.85	0.50	no	550	814	435	7.48	0.50	no	—	564	310
1/3 T turbine	1.85	0.50	yes	335	683	395	7.48	0.50	yes	—	472	281
1/2 T turbine	1.85	0.25	no	—	420	148	7.48	0.25	no	—	292	106
1/2 T turbine	1.85	0.25	yes	130	352	134	7.48	0.25	yes	85	244	96
1/2 T turbine	1.85	0.50	no	—	597	164	7.48	0.50	no	—	414	117
1/2 T turbine	1.85	0.50	yes	140	500	149	7.48	0.50	yes	—	347	106
1/3 T pitch b.	1.85	0.25	no	—	—	839	7.48	0.25	no	—	—	597
1/3 T pitch b.	1.85	0.25	yes	580	—	762	7.48	0.25	yes	420	—	542
1/3 T pitch b.	1.85	0.50	no	—	—	928	7.48	0.50	no	—	—	661
1/3 T pitch b.	1.85	0.50	yes	620	—	843	7.48	0.50	yes	—	—	600
1/2 T pitch b.	1.85	0.25	no	—	—	283	7.48	0.25	no	—	—	202
1/2 T pitch b.	1.85	0.25	yes	195	—	257	7.48	0.25	yes	115	—	184
1/2 T pitch b.	1.85	0.50	no	—	—	313	7.48	0.50	no	—	—	224
1/2 T pitch b.	1.85	0.50	yes	270	—	284	7.48	0.50	yes	—	—	203

0.25, are collected. The results on a 1.85 dm^3 scale concerning the effects of temperature and the presence of polymer particles in the system are confirmed by the results on a 7.48 dm^3 scale.

The results given in the Tables III and IV reveal a significant influence of the impeller type and diameter on N^*. In agreement with Johansson and Godfrey,[28] our results show that the Rushton turbine impeller required less power per unit of mass than the pitch-blade impeller under the same conditions. The different performance of the impellers used was more pronounced on the larger scale. The results indicate that using a Rushton turbine instead of a pitched-blade impeller, as well as using a larger impeller diameter, provides better emulsification at constant average power input per unit of mass. Note that the torque on the impeller shaft determined on a 1.85 dm^3 scale has a limited accuracy. This limited accuracy originates from the low absolute value of the torque. Consequently, the difference between "measured" and "calculated" mean energy dissipation is significantly larger than on the 7.48 dm^3 scale where this difference is smaller, because of the better accuracy of the torque measurement.

The pitched blade and turbine impellers generate completely different flow patterns (see Fig.e 1), and, consequently, the energy dissipation distribution in the vessel will be different. However, the circulation time, calculated with eq. (11) and the experimentally determined N^*, does not show remarkable distinctions between the impellers.

The results of the various scale-up rules for N^* on scaling up from the 1.85 dm^3 to the 7.48 dm^3 are presented in Table V. In Table V the experimentally observed values of N^* on both scales are also given. The underlined stirrer speed gives the closest approach to the experimentally determined value of N^* on the 7.48 dm^3 scale for a particular system. Scaling up with constant Reynolds number and constant power input always underestimates N^* , while the other scale-up rules overestimate N^* in most cases. Considering the turbine impeller, scale-up based on constant impeller tip speed appears to be most appropriate. The scale-up of N^* for the pitched-blade impeller is more complicated, although scale-up with constant impeller tip speed gives a rough estimate. To make sure no mass transfer limitations occur during polymerization with a pitched-blade impeller, it is recommended to keep the mean energy dissipation constant for predicting the lowest impeller speed for sufficient emulsification.

Table VII Constants Used for the Calculation of N^* According to Eqs. (4) and (5)

g (m/s^2)	9.81
σ (N/m) without emulsifier	0.012
σ (N/m) with emulsifier	0.0012
ρ_{water} (kg/m^3)	1000
$\rho_{styrene}$ (kg/m^3)	878
$\rho_{mixture}$ (kg/m^3)[15]	$(1 - \phi_v)\ \rho_c + \phi_v \rho_d$
μ_{water} [Pa s]	$1.00 \cdot 10^{-3}$
$\mu_{styrene}$ [Pa s]	$0.691 \cdot 10^{-3}$
$\mu_{mixture}$ [Pa s][15]	$\frac{\mu_c}{1 - \bar{3}\phi_v}\left(1 + \frac{1.5\ \mu_d \phi_v}{\mu_d + \mu_c}\right)$
C‴ (−) turbine[15]	0.53
α (−) turbine[15]	1.7
C‴ (−) pitched blade[15]	0.84
α (−) pitched blade[15]	1.97

In Table VI, the prediction of N^*, calculated with the empirical eqs. (4) and (5), respectively, reported by Van Heuven and Beek[13] and Skelland and Ramsay,[14] are given for the experimental setup used in this study. The physical constants used, have been collected in Table VII. For both equations, the trends in terms of impeller type and impeller diameter are in qualitative agreement with the experimentally observed values of N^*. The effect of monomer fraction in the recipe on N^* is overestimated by both eqs. (4) and (5) in all cases. The eqs. (4) and (5) underestimate the influence of emulsifier as expressed in the interfacial tension σ. The equation, developed by Skelland and Ramsay,[14] approaches the experimentally observed N^* closer than the relation given by van Heuven and Beek.[13] In general, eq. (5) gives a rough estimate of the lowest impeller speed necessary for sufficient emulsification of a particular system.

Polymerization Experiments

Several ab initio experiments of the emulsion polymerization of styrene, with varying impeller speeds were performed (see Table VII and Fig. 3). Figure 3 shows that there is an impeller speed above which no significant change in conversion time history can be observed. This is the same impeller speed as N^* for the particular system. For the experiments shown in Figure 3, $N^* = 360$ rpm. During the polymerization experiments with a stirrer speed below N^*, the emulsification was not sufficient. Although in interval I no significant difference in results could be observed compared to the experiments at higher stirrer speeds, in interval II the conversion and particle size deteriorated.

Table VIII Characteristics of the *Ab Initio* Emulsion Polymerization Experiments of Styrene

Impeller Type	Scale (dm^3)	$C_{E,ov}$ (kmol/m_w^3)	N_i (rpm)	T_r (°C)	T_q (Nm)	$\varepsilon_{av,m}$ (W/kg)	$\varepsilon_{av,c}$ (W/kg)	t_c (s)	X_{final} (−)	$d_{pv,final}$ (nm)	PSD	Emulsification
1/3 T turbine	1.85	0.02	250	50.0	—	—	0.034	2.3	0.38	57	Broad/bimodal	Insufficient
1/3 T turbine	1.85	0.02	275	50.0	0.0096	0.15	0.045	2.1	0.70	60	Broad/bimodal	Insufficient
1/3 T turbine	1.85	0.02	275	50.0	0.0050	0.078	0.045	2.1	0.80	69	Broad	Insufficient
1/3 T turbine	1.85	0.02	360	50.0	0.0094	0.19	0.10	1.6	0.95	72	Normal	N^*
1/3 T turbine	1.85	0.02	500	50.0	0.0088	0.25	0.27	1.1	0.94	70	Normal	Good
1/3 T turbine	1.85	0.02	800	50.0	0.027	1.2	1.1	0.7	0.90	73	Normal	Good
1/3 T turbine	1.85	0.02	370	75.0	0.0085	0.18	0.11	1.5	0.96	62	Slight broader	Good
1/2 T pitch b.	1.85	0.02	195	50.0	0.0083	0.092	0.049	1.4	0.86	71	Slightly broader	N^*
1/2 T pitch b.	1.85	0.02	195	50.0	0.0079	0.087	0.049	1.4	0.91	79	Slightly broader	N^*
1/2 T pitch b.	1.85	0.02	235	50.0	0.0117	0.16	0.085	1.2	0.92	88	Slightly broader	N^*_{seeded}
1/2 T pitch b.	1.85	0.02	210	75.0	0.0098	0.12	0.061	1.3	0.96	61	Slightly broader	N^*
1/3 T turbine	7.48	0.01	205	50.0	0.018	0.052	0.042	2.7	0.71	81	Slightly broader	N^*
1/3 T turbine	7.48	0.01	450	50.0	0.087	0.55	0.45	1.2	0.90	91	Normal	Good
1/3 T turbine	7.48	0.02	205	50.0	0.022	0.063	0.042	2.7	0.92	81	Normal	$N^*_{CE=0.01}$
1/3 T turbine	7.48	0.02	450	50.0	0.087	0.55	0.45	1.2	0.96	90	Normal	Good

Figure 4 shows the corresponding particle size distributions of the final latices of the experiments shown in Figure 3. The particle size distribution of the experiment with N_i = 275 rpm is very broad. Due to mass transfer limitation of monomer, the interval of particle nucleation lasts longer than for polymerization with negligible mass transfer limitations. The particles grow slowly, the consumption of emulsifier by adsorption onto the particle surface is limited, and consequently, more micelles are present over a longer period of time. The particle size distributions of the experiments with N_i = 360, 500, and 800 rpm are approximately the same.

Figure 5 shows the effect of temperature and impeller type on the ab initio emulsion polymerization of styrene with a stirrer speed equal to N^* in all cases. At 50°C reaction temperature, the conversion time history of the experiment with the pitched blade impeller of D = 1/2 T shows a significant deviation from the conversion time history of the experiment with the Rushton turbine impeller of D = 1/3 T. Apart from some effects by traces of oxygen left in the reaction mixture, this difference might indicate some mass transfer limitation during the polymerization with the pitched blade impeller. The particle size curves of both experiments, however, show little difference. The particle size distribution of the polymerization with the pitched blade impeller broadened hardly compared to the particle size distributions of Figure 4(B), (C), and (D). The molecular weight distribution was identical to the molecular weight distributions of the turbine impeller experiments with N_i = 360 and 800 rpm.

The mass transfer limitation for the experiment with the pitched blade impeller might not be so severe as in case of the turbine impeller with N_i = 275 rpm (see Fig. 3), but the visually determined N^* = 195 rpm for the pitched blade impeller with 1/2 T, did not completely guarantee intrinsic polymerization.

At 75°C reaction temperature, the differences in conversion time history and particle size development between the turbine and pitch blade impeller are not significant. The higher reaction temperature did increase the polymerization rate compared to the 50°C polymerization, but the visually determined N^* is for both impellers sufficient to guarantee intrinsic polymerization.

In Figure 6(A) the results of several ab initio emulsion polymerization experiments of styrene on the 7.48 dm^3 scale are presented. For an equal emulsifier concentration of 0.02 kmol/m_w^3, both the 7.48 dm^3 experiments follow the curve fit of the conversion time history on the 1.85 dm^3 scale. No difference in conversion time history between the two experiments on the 7.48 dm^3 scale is observed. The results indicate that on a 7.48 dm^3 scale no significant influence of the impeller speed on the conversion time history can be expected for $N_i > N^*$.

The evolution of the particle size with time for the experiments on the 7.48 dm^3 scale has been presented in Figure 6(B). The results in Figure 6(B) reveal that the mean particle size on the 7.48 dm^3 scale deviates from that observed on a 1.85 dm^3 scale and intrinsic polymerization. The deviation is significant for reaction times longer than

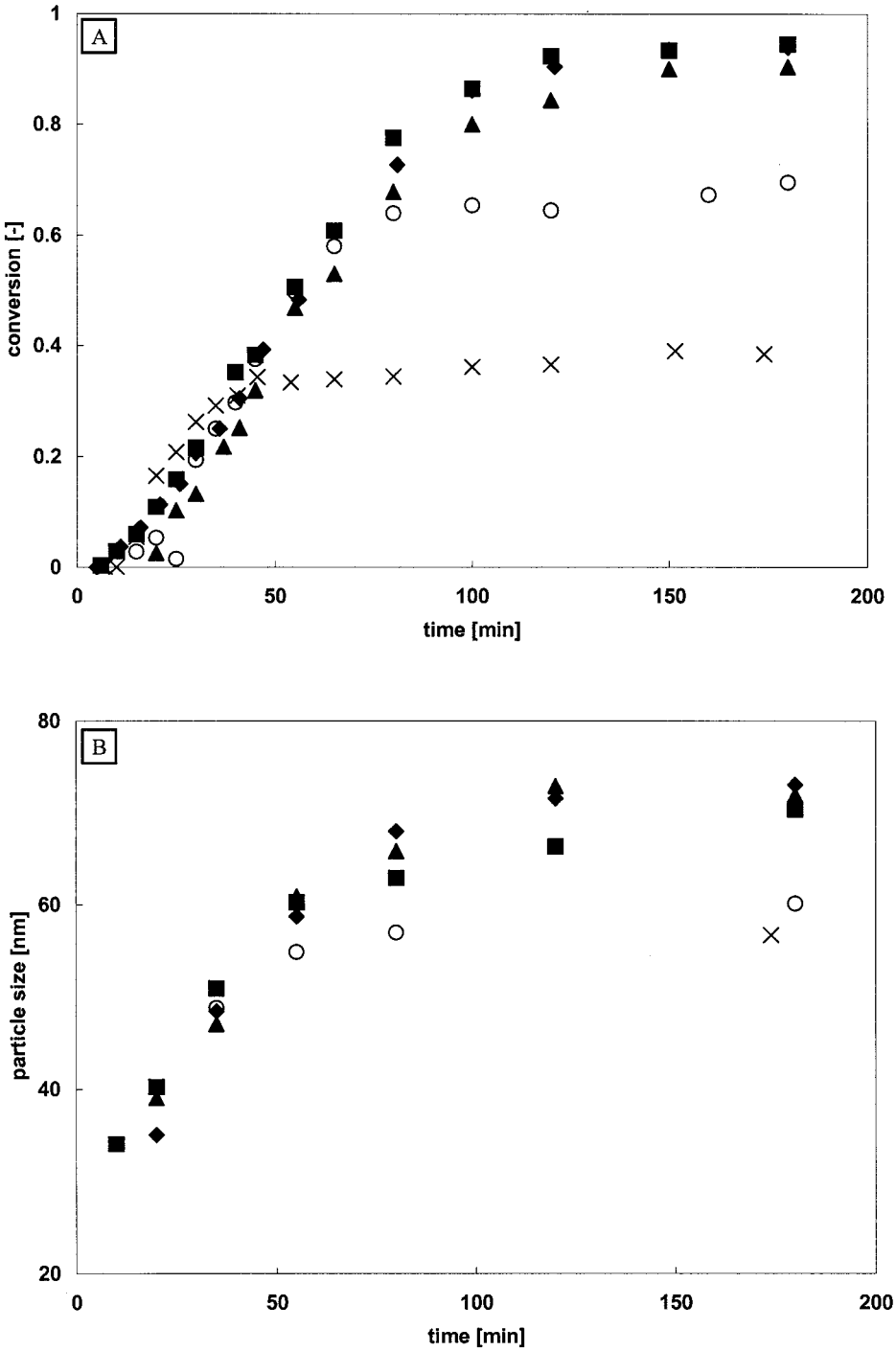

Figure 3 Ab initio emulsion polymerization experiments of styrene with a Rushton turbine impeller 1/3 T on a 1.85 dm^3 scale. (A) Conversion time history, (B) Particle size versus time. $C_{E,\mathrm{ov}}$ = 0.02 kmol/m_w^3, T_r = 50.0°C, ϕ_M = 0.25, 1.85 dm^3 scale. Stirrer speed [rpm]: ×: 250; ○: 275; ■: 360 (N*); ◆: 500; ▲: 800.

40 min. The evolution of the particle size for small-scale experiments is given by a curve fit for experiments with intrinsic polymerization [see Fig. 3(B)].

At a low emulsifier concentration of 0.01 kmol/m_w^3, some influence of impeller speed on the conversion time history was observed [see Fig. 6(A)]. The conversion of the experiment with $N_i = N$* is

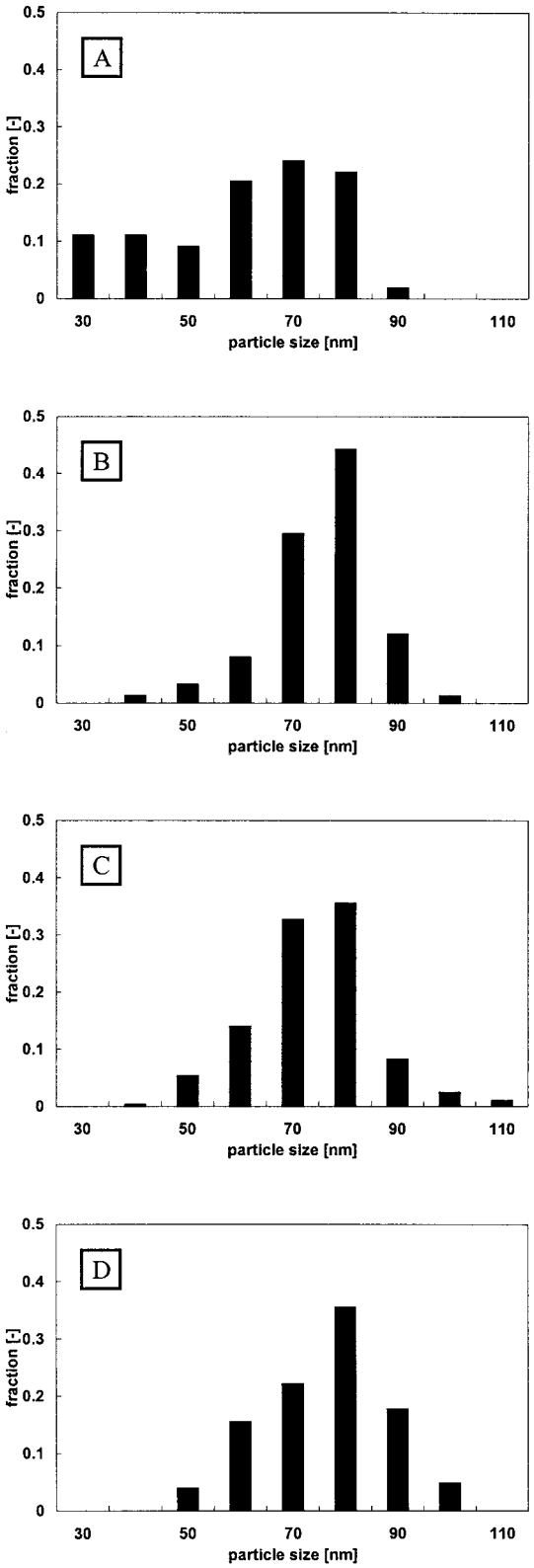

Figure 4 Particle size distribution of final latices of the polymerization experiments with Rushton turbine impeller of 1/3 T on 1.85 dm^3 scale. (A) N_i = 275 rpm, X_{final} = 0.70; (B) $N_i = N^*$ = 360 rpm, X_{final} = 0.05; (C) N_i = 500 rpm, X_{final} = 0.94; (D) 800 rpm, X_{final} = 0.91.

somewhat different from that of the experiment with $N_i > N^*$, and the particle size distribution of the former experiment is slightly broader. Although according to the visualization experiments, N^* = 205 rpm, during emulsion polymerization some mass transfer limitation of monomer occurs. At low emulsifier concentration, close to the critical micelle concentration, the stirrer is probably less efficient in breaking up the monomer droplets into smaller ones. Consequently, the overall surface of the monomer droplets for mass transfer is smaller than at high emulsifier concentration. The polymerization rate increased with emulsifier concentration, however, not as predicted by eq. (12).

If ab initio emulsion polymerization experiments with a pitched blade impeller of D = 1/3 T with $N_i = N^* =$ 195 rpm and $N_i = N^*_{\text{seeded}}$ = 235 rpm are compared, the results indicate that the latter polymerization proceeded slightly faster. However, before further conclusions can be drawn a future detailed study based on reaction calorimetry is needed.

Comparing the duplicate experiments of the pitched blade impeller with N_i = 195 rpm and the turbine impeller with N_i = 275 rpm, respectively, emphasize that besides emulsification, other effects, such as different levels of oxygen in the reaction system may influence the course of the reaction.

CONCLUSIONS

In conclusion, the results of this study on emulsification in batch emulsion polymerization of styrene reveal that the lowest impeller speed for sufficient emulsification, as determined by visualization tests, in most cases corresponds with the impeller speed above which intrinsic polymerization occurs.

Concerning the impeller type and diameter as well as the physicochemical properties of the liquid–liquid mixture, the following conclusions can be drawn: (1) using a turbine impeller instead of a pitched-blade impeller results in less power input for providing sufficient emulsification. (2) A larger impeller diameter requires less power input for proper emulsification.

Considering the turbine impeller, a scale-up rule of the lowest impeller speed for proper emulsification, N^*, based on constant impeller tip speed appears to be most appropriate.

The scale-up rule for the pitched-blade impeller is more complicated. It is recommended to

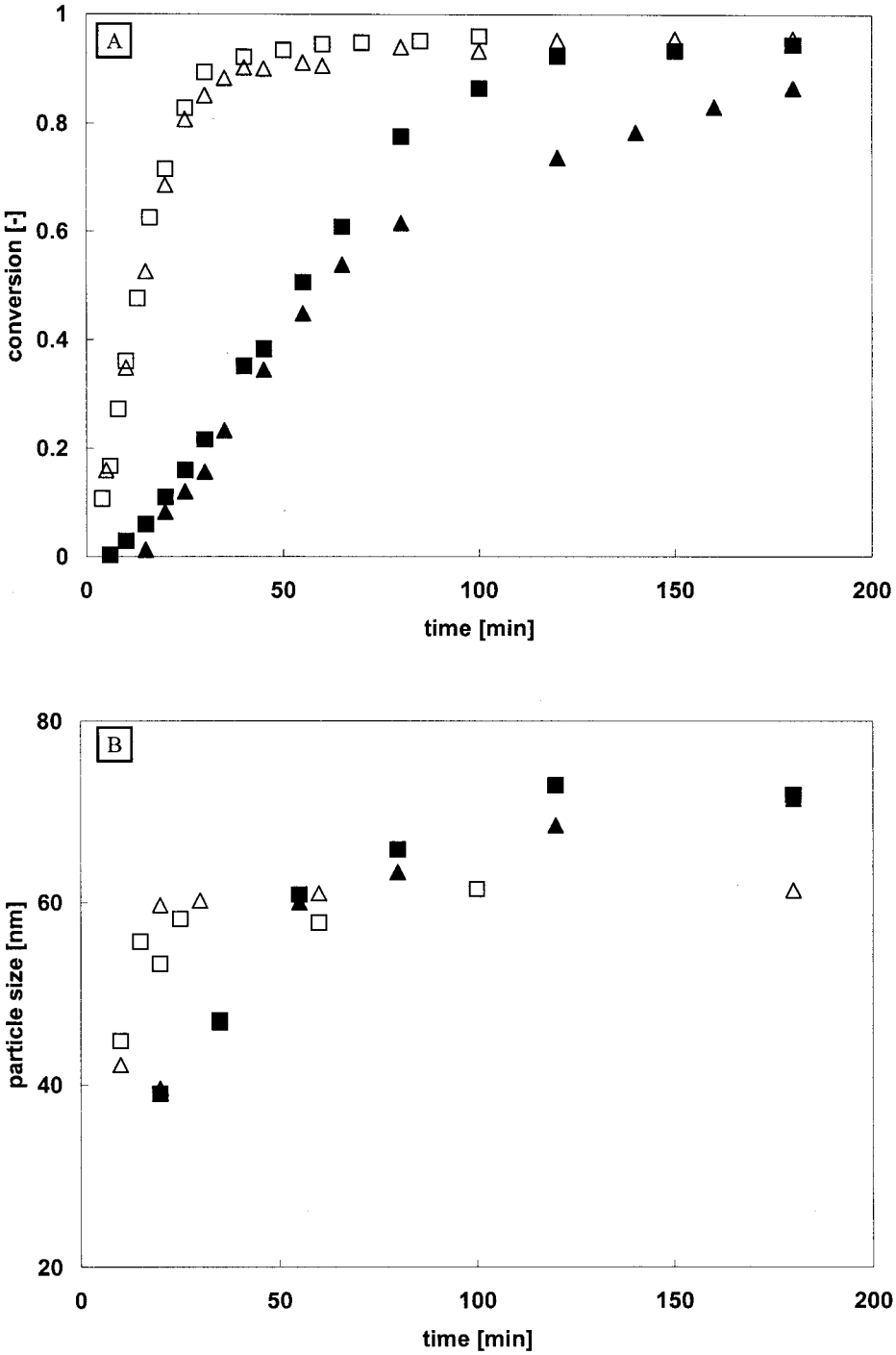

Figure 5 Ab initio emulsion polymerization experiments of styrene with varying impeller type and reaction temperature. (A) Conversion time history, (B) particle size versus time. $C_{E,ov}$ = 0.02 kmol/m_w^3, ϕ_M = 0.25, a 1.85 dm^3 scale. ■: 1/3 T turbine impeller, N_i = 360 rpm (N*), T_r = 50.0°C; ▲: 1/2 T pitched blade impeller, N_i = 195 rpm (N*), T_r = 50.0°C; □: 1/3 T turbine impeller, N_i = 370 rpm (N*), T_r = 75.0°C; △: 1/2 T pitched-blade impeller, N_i = 210 rpm (N*), T_r = 75.0°C.

keep the mean energy dissipation constant. (3) Addition of emulsifier to the mixture considerably decreases N*. (4) At elevated temperatures, the coalescence rate of the monomer droplets is higher and consequently N* increases. (5) Introduction of polymer particles in the mixture increases N*. (6)

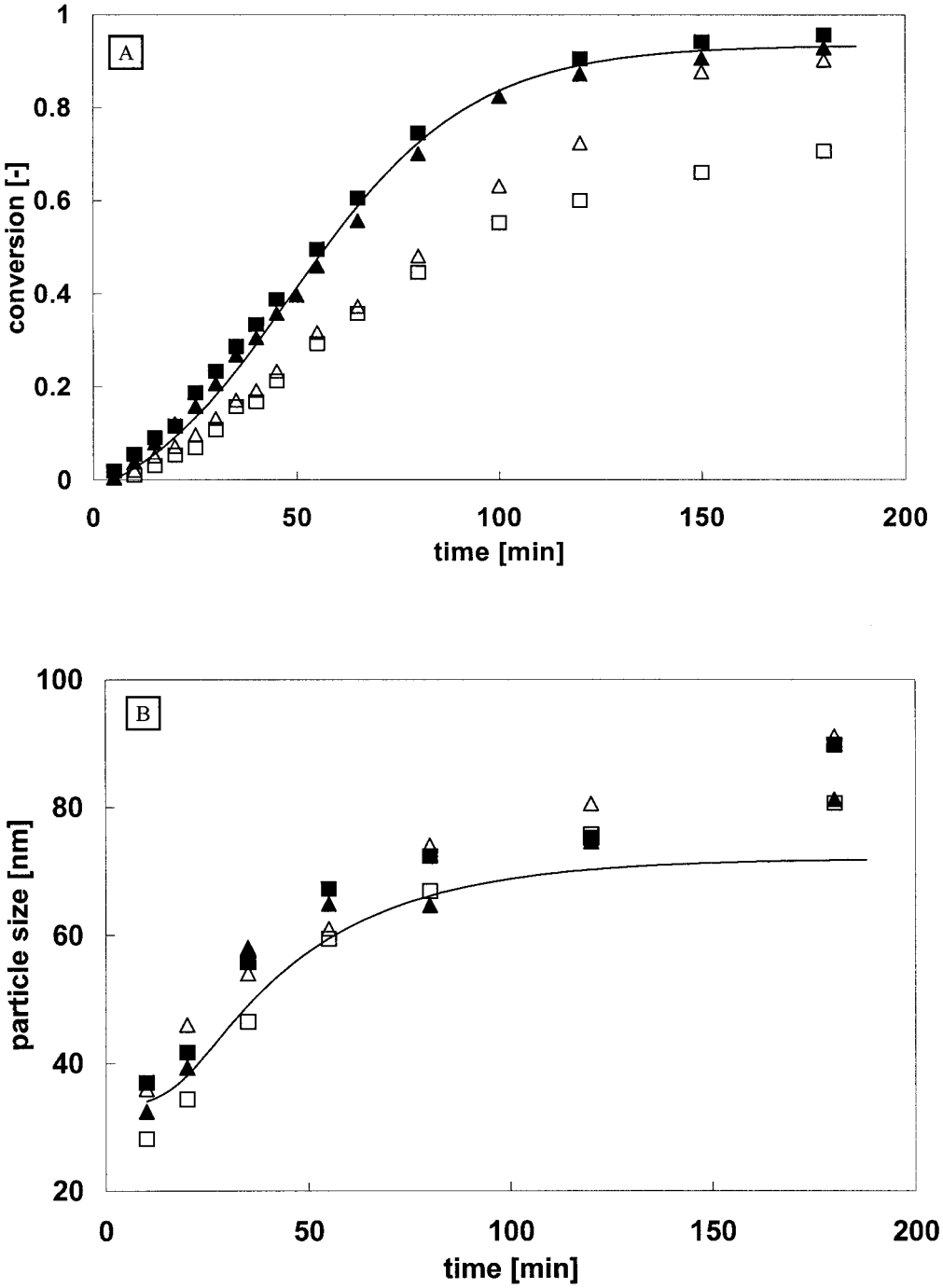

Figure 6 Ab initio emulsion polymerization experiments of styrene with varying impeller speed and emulsifier concentration. (A) Conversion time history; (B) particle size versus time. Rushton turbine impeller with $D = 1/3\ T$, $T_r = 50.0°C$, $\phi_M = 0.25, 7.48$ dm^3 scale. ■: $C_{E,ov} = 0.02$ kmol/m_w^3, $N_i = 205$ rpm (N^*); ▲: $C_{E,ov} = 0.02$ kmol/m_w^3, $N_i = 450$ rpm; □: $C_{E,ov} = 0.01$ kmol/m_w^3, $N_i = 205$ rpm (N^*); △: $C_{E,ov} = 0.01$ kmol/m_w^3, $N_i = 450$ rpm; —: curve fit of polymerization experiments with turbine impeller of 1/3 T with impeller speed 360, 500, and 800 rpm on a 1.85 dm^3 scale (see Fig. 3).

The empirical equation reported by Skelland and Ramsay (1987) provides a rough estimate of N^* for a particular system.

The authors thank the Foundation Emulsion Polymerization (SEP) for the financial support of this study, and P. C. M. van Loon for his contribution to

this work. We acknowledge the useful comments by Prof. D. Thoenes.

NOTATION

C	clearance of impeller from tank bottom (m)
C'	constant for maximum droplet size eq. (2) (−)
C''	constant for minimal droplet size eq. (3) (−)
C'''	constant for N^* eq. (5) (−)
C_{CMC}	critical micelle concentration (kmol/m_w^3)
$C_{E,ov}$	overall emulsifier concentration (kmol/m_w^3)
C_{I0}	initial initiator concentration (kmol/m_w^3)
C_{M0}	initial monomer concentration (kmol/m_w^3)
D	impeller diameter (m)
d	droplet size (m)
d_{max}	maximum stable droplet size before break up occurs (m)
d_{min}	minimal stable droplet size before coalescence occurs (m)
$d_{p,v,final}$	volume averaged diameter of final latex (m)
F	interaction force between two droplets (N)
g	acceleration due to gravity (m/s^2)
H	height of reactor (m)
H_{fill}	height of reactor filled with liquid (m)
l	impeller blade length (m)
M_M	mass of liquid–liquid mixture (kg)
N_c	circulation number (−)
N_i	rotational impeller speed (1/s)
N^*	lowest impeller speed for proper emulsification (1/s)
N^*_{seed}	lowest impeller speed for proper emulsification with polymer particles present in the mixture (1/s)
N_P	power number (−)
N_{part}	particle number (1/m_w^3)
P	power input (W)
R_p	reaction rate (mol/m_w^3 s)
t	time (s)
T_q	torque (N m)
t_c	circulation time (s)
T_r	reaction temperature (°C)
T	internal tank diameter (m)
$u^2(d)$	mean square of relative velocity fluctuations between two diametrically opposite points on the surface of droplets (m^2/s^2)
V_M	volume of liquid–liquid system (m^3)
w	impeller blade width (m)
We	Weber number (−)
X_{final}	conversion of final latex (kg/kg)

Greek

α	constant of N^* equation, characteristic for impeller type (5) (−)
β	exponent of relation between droplet size and mean energy dissipation [eq. (10) (−)]
ε_{av}	mean energy dissipation (W/kg)
$\varepsilon_{av,m}$	mean energy dissipation, based on the torque measured on the impeller shaft [eqs. (6) and (9)] (W/kg)
$\phi_{av,c}$	mean energy dissipation, calculated with the power number [eqs. (7) and (9)] (W/kg)
ϕ_M	mass fraction of monomer in the mixture (−)
ϕ_V	volume fraction of monomer in the mixture (−)
$\Phi(\mu_d/\mu_c)$	function dependent on the ratio of dynamic viscosity of continuous and dispersed phase (−)
μ_c	dynamic viscosity of continuous phase (Pa s)
μ_d	dynamic viscosity of dispersed phase (Pa s)
μ_M	dynamic viscosity of liquid–liquid mixture (Pa s)
η_c	kinematic viscosity of continuous phase (m^2/s)
ρ_c	density of continuous phase (kg/m^3)
ρ_M	density of liquid–liquid system (kg/m^3)
$\Delta\rho$	difference in density between continuous and dispersed phase (kg/ m^3)
σ	Interfacial tension (N/m)

REFERENCES

1. Harkins, W. D. J Am Chem Soc 1947, 69, 1428.
2. Smith, W. V.; Ewart, R. H. J Chem Phys 1948, 16, 592.
3. Gilbert, R. G. Emulsion Polymerization, a Mechanistic Approach; Academic Press: New York, 1995.
4. Becher, P. Emulsions, Theory and Practice; Reinhold Publishing Corporation: New York, 1977, 2nd ed.
5. Hinze, J. O. AIChE J 1955, 1, 289.
6. Shinnar, R. J Fluid Mech 1961, 10, 259.
7. Baldyga, J.; Podgorska, W.; Smit, L. Proc. 9th Eur Mixing Conf 1997, 11, 247.
8. Sprow, F. B. Chem Eng Sci 1967, 22, 435.

9. Pacek, A. W.; Man, C. C.; Nienow, A. W. Proc. 9th Eur Mixing Conf 1997, 11, 263.
10. Ivanov, I. B. Pure Appl Chem 1980, 52, 1241.
11. Sprow, F. B. AIChE J 1967, 13, 995.
12. Skelland, A. H. P.; Seksaria, R. Ind Eng Chem Proc Des Dev 1978, 17, 56.
13. van Heuven, J. W.; Beek, J. W. Proc Int Solv Extr Conf 1971, paper 51.
14. Skelland, A. H. P.; Ramsay, G. G. Ind Eng Chem Res 1987, 26, 77.
15. Skelland, A. H. P.; Moeti, L. T. Ind Eng Chem Res 1989, 28, 122.
16. Bates, R. L.; Fondy, P. L.; Corpstein, R. R. I&EC Proc Des Dev 1963, 2, 310.
17. Salager, J. L.; Perez-Sanchez, M.; Raminez-Gouveia, M.; Anderez, J. M.; Briceno-Rivas, M. I. Proc 9th Eur Mixing Conf 1997, 11, 123.
18. Okamoto, Y.; Nishikawa, M.; Hashimoto, K. Int Chem Eng 1981, 21, 88.
19. Wu, H.; Patterson, G. K. Chem Eng Sci 1989, 44, 2207.
20. Schäfer, M.; Yianneskis, M.; Wächter, P.; Durst, F. AIChE J 1998, 44, 1233.
21. Thoenes, D. Chemical Reactor Development, From Laboratory to Industrial Production; Kluwer Academic Publishers: New York, 1994.
22. Esch, D. D.; D'Angelo, P. J.; Pike, R. W. Can J Chem Eng 1971, 49, 872.
23. Zhou, G.; Kresta, S. M. Chem Eng Sci 1998, 53, 2063.
24. Zhou, G.; Kresta, S. M. Chem Eng Sci 1998, 53, 2099.
25. Hoedemakers, G. F. M. PhD Thesis, Eindhoven University of Technology (1990).
26. van den Boomen, F. H. A. M.; Akhssay, M. Internal report Laboratory of Process Development, Eindhoven University of Technology (1997).
27. Nomura, M.; Harada, M.; Eguchi, W.; Nagata, S. J Appl Polym Sci 1972, 16, 835.
28. Johansson, A. C.; Godfrey, J. C. Proc 9th Eur Mixing Conf 1997, 11, 255.